

## Supplementary Information

Using optical tweezer electrophoresis to investigate clay  
nanoplatelet adsorption on Latex microspheres in aqueous media

Vaibhav Raj Singh Parmar<sup>1</sup>, Sayantan Chanda<sup>1</sup>, Sri Vishnu Bharat Sivasubramaniam<sup>1</sup>, and  
Ranjini Bandyopadhyay<sup>1,\*</sup>

<sup>1</sup>*Soft Condensed Matter Group, Raman Research Institute, C. V. Raman Avenue,  
Sadashivanagar, Bangalore 560 080, INDIA*

January 6, 2025

---

\*Corresponding Author: Ranjini Bandyopadhyay; Email: ranjini@rri.res.in

ST1 Cryogenic field emission scanning electron microscopy (cryo-FESEM) images of Latex microsphere

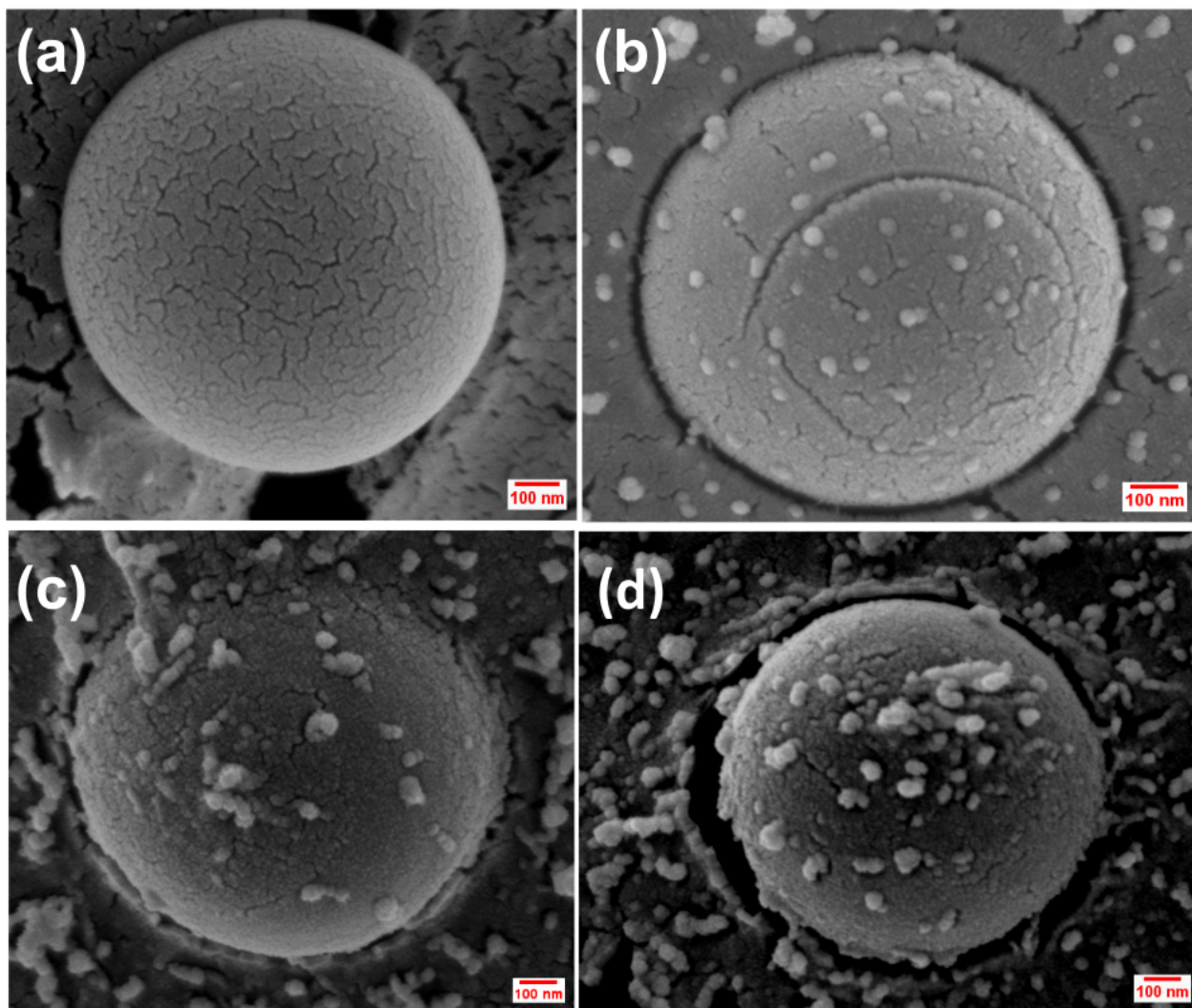


Fig. S1: Raw cryo-FESEM images of a trapped Latex microsphere in (a) pure water, (b) an aqueous Laponite suspension of concentration 2.5% w/v, (c) an aqueous 2.5% w/v Laponite suspension with 1.25 mM NaCl and (d) an aqueous 2.5% w/v Laponite suspension with 1.25 mM TSPP.

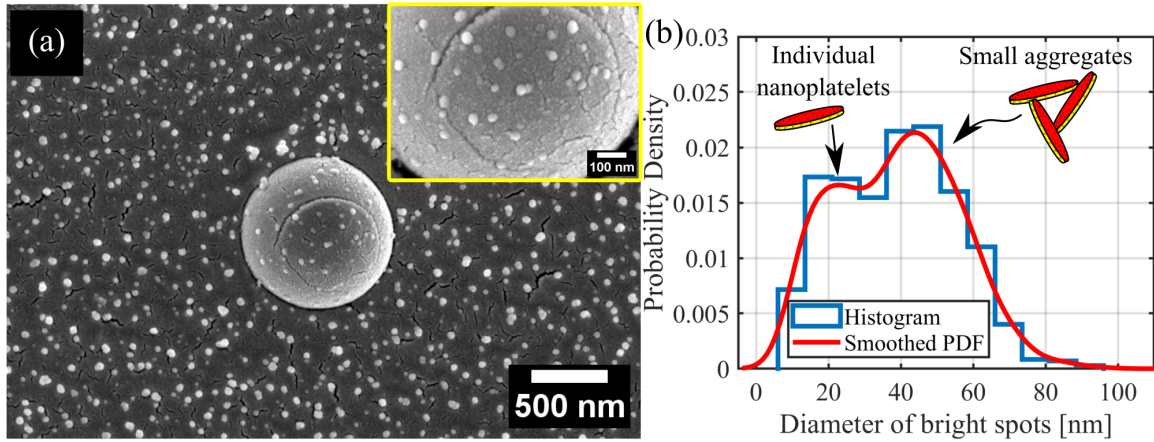


Fig. S2: (a) Cryo-FESEM image of a Latex microsphere (diameter = 1  $\mu\text{m}$ ) suspended in a clay suspension of concentration 2.5% w/v at aging time  $t_w = 90$  minutes. (Inset) Higher magnification image of the Latex microsphere surface. Many bright spots can be seen on the surface of the microsphere. (b) Histogram and smoothed probability density of the diameters of 932 bright spots identified from (a) using ImageJ and estimated using the histogram and ksdensity functions in MATLAB@2024. The diameter of each bright spot was estimated from its area,  $A_{spot}$ , by calculating  $2\sqrt{A_{spot}/\pi}$ . The peak in the probability density function at  $\sim 25$  nm corresponds to an individual clay nanoplatelet, while the second peak at a larger diameter corresponds to small clay aggregates

## ST2 Calibrations of the optical tweezer

### ST2.1 Measurement of calibration factor $\beta$

The QPD output gives the differential voltages  $V_x = V_1 - V_2 - V_3 + V_4$ ,  $V_y = V_1 + V_2 - V_3 - V_4$ , and the sum voltage  $V_S = V_1 + V_2 + V_3 + V_4$ , where  $V_{1-4}$  are diode voltages. The differential voltages  $V_x$  and  $V_y$  were normalised by  $V_S$  prior to estimating the calibration factor  $\beta$ .

The calibration factor,  $\beta$ , determined from the uncalibrated power spectrum,  $S_{vv}$ , of the trapped microsphere is related to the position of the microsphere as follows:  $x = \beta x_v$ , where  $x_v = V_x/V_S$  is the dimensionless position of the microsphere. Therefore,  $\beta$  has units of distance. The power spectrum of the particle is given by:

$$S_{xx} = \frac{1}{T} \int_0^T e^{-i\omega t} \int_0^T x(t)x(t+\tau) d\tau dt \quad (\text{S1})$$

Therefore,  $S_{xx} = \beta^2 S_{vv}$ . For a trapped Brownian particle,  $S_{xx}$  is theoretically calculated from the first term in Eqn. (2) of the main manuscript:

$$S_{xx} = \beta^2 S_{vv} = \frac{k_B T}{\pi^2 \gamma (f_c^2 + f^2)} \quad (\text{S2})$$

For frequencies  $f \gg f_c$ ,

$$f^2 S_{vv} = \beta^{-2} \frac{k_B T}{\pi^2 \gamma} \quad (\text{S3})$$

This indicates that  $f^2 S_{vv}$  attains a constant value at high frequencies. For a microsphere trapped in water, the plateau is clearly visible in Fig. S3(a). Since the Stokes drag coefficient  $\gamma = 6\pi\eta a$ , where  $a = 0.5 \mu\text{m}$  is the radius of the microsphere,  $\eta = 0.89 \text{ mPa}\cdot\text{s}$  is the medium viscosity and  $T = 22^\circ\text{C}$  is the temperature of the medium, the calibration factor,  $\beta$ , can be determined using Eqn. (S3). This method is less prone to errors as the possibility of experimental noise at lower frequencies is eliminated. Calibration factor,  $\beta$ , evaluated at various laser powers at the back aperture of the objective lens, is plotted in Fig. S3(b).

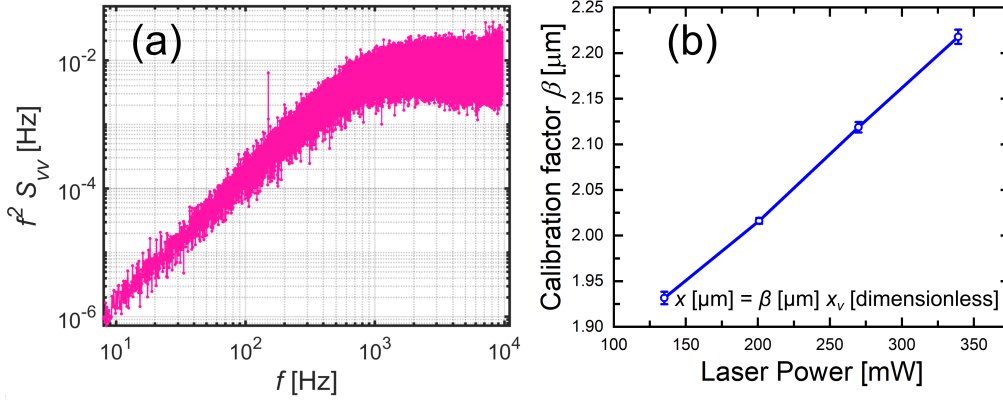


Fig. S3: (a)  $f^2 S_{vv}$  as a function of  $f$  for a microsphere trapped in water. (b) Calibration factor,  $\beta$  vs. laser power. The laser powers were measured at the back aperture of the objective lens. The error bars represent the standard errors estimated from 11 microspheres trapped in water. We note that  $\beta$  has units of distance instead of distance/volts as normalised QPD outputs were used for analysis.

## ST2.2 Calculation of power spectral density (PSD) from the position fluctuations of a trapped Brownian microsphere

Figure S4(a) shows the thermal fluctuations of a microsphere optically trapped in water. We acquired the time-dependent position fluctuations of the optically trapped microsphere for a period of 70 minutes. We divided this data into equally-spaced datasets containing position fluctuations acquired for 80 seconds. The dataset containing position fluctuations for 80 seconds was further divided into 10 sub-datasets with equally-spaced data. The power spectral density (PSD) for each sub-dataset was estimated using the periodogram function in MATLAB as shown by grey curves in Fig. S4(b). 10 power spectral density curves were extracted to compute an average (black circles in Fig. S4(b)). Since there can be noise and aliasing effects at low and high frequencies, power spectral densities in a frequency range of 10 to 11000 Hz were used for further analysis (Figs. S4(c,d)). The peak observed near 200 Hz in Figs. S4(c,d) was identified as environmental noise from the laboratory and eliminated. Despite carefully positioning the sample cell on the sample holder, a slight misalignment still existed between the direction of the applied field and the horizontal axis of the QPD. The slight misalignment resulted in a weak peak at  $f = f_{AC}$  in the PSD along the  $\hat{y}$ -direction. We resolved this issue during data analysis by rotating the position fluctuation data until the electric field direction was perfectly aligned with the horizontal axis of the QPD. This reduces complexity in further analysis.

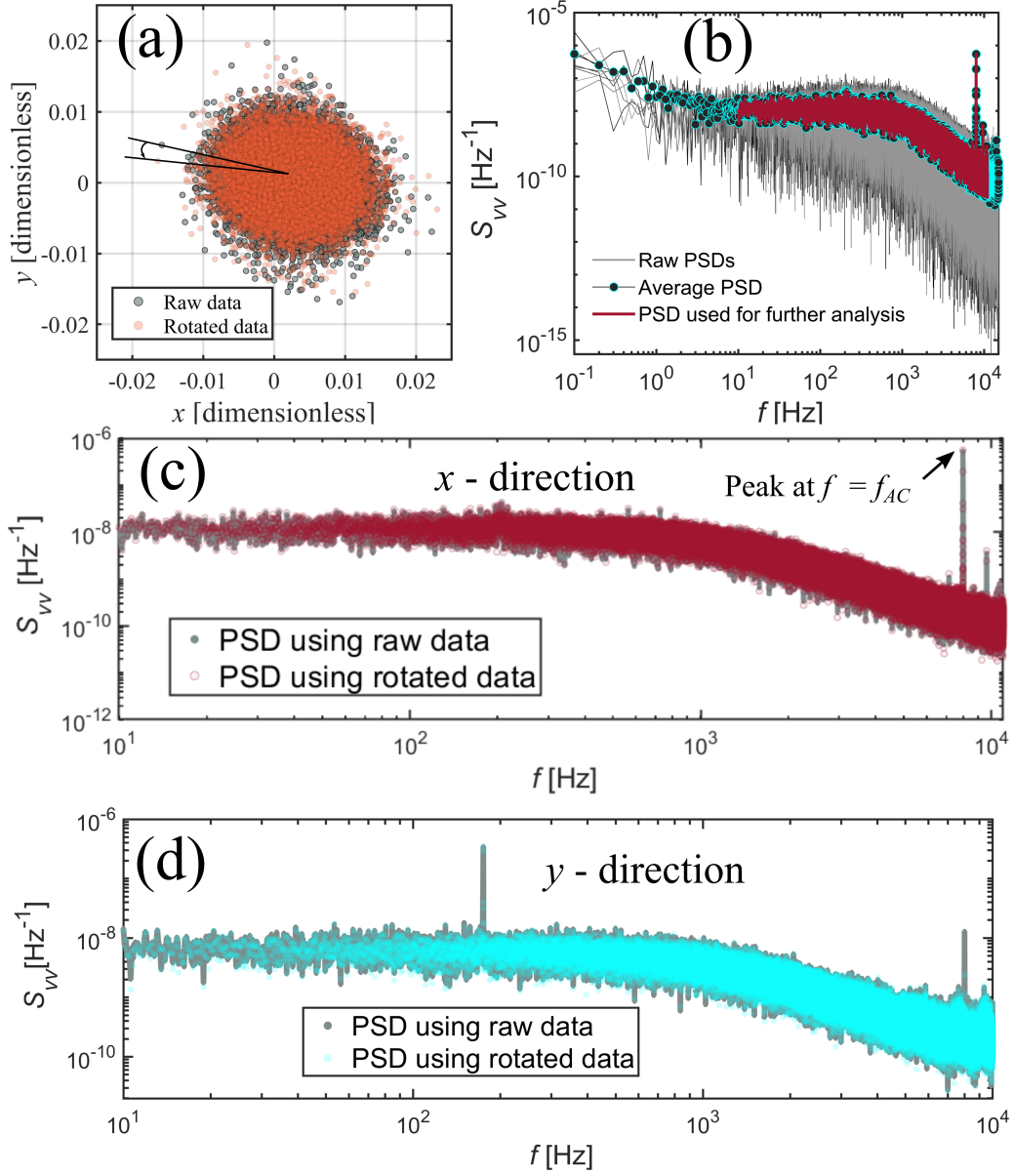


Fig. S4: (a) Scatter plot showing position fluctuations of the trapped microsphere. The data is rotated by an angle  $< 0.15$  rad to align the electric field with the horizontal axis of the QPD. (b) Power spectral densities of individual sub-datasets, average power spectral density, and cropped power spectral density used for further analysis. (c,d) Power spectral densities along  $\hat{x}$  and  $\hat{y}$  directions respectively, computed from raw and rotated position fluctuations. It is seen from (d) that rotation eliminates the  $f = f_{AC}$  peak from the  $\hat{y}$ -direction.

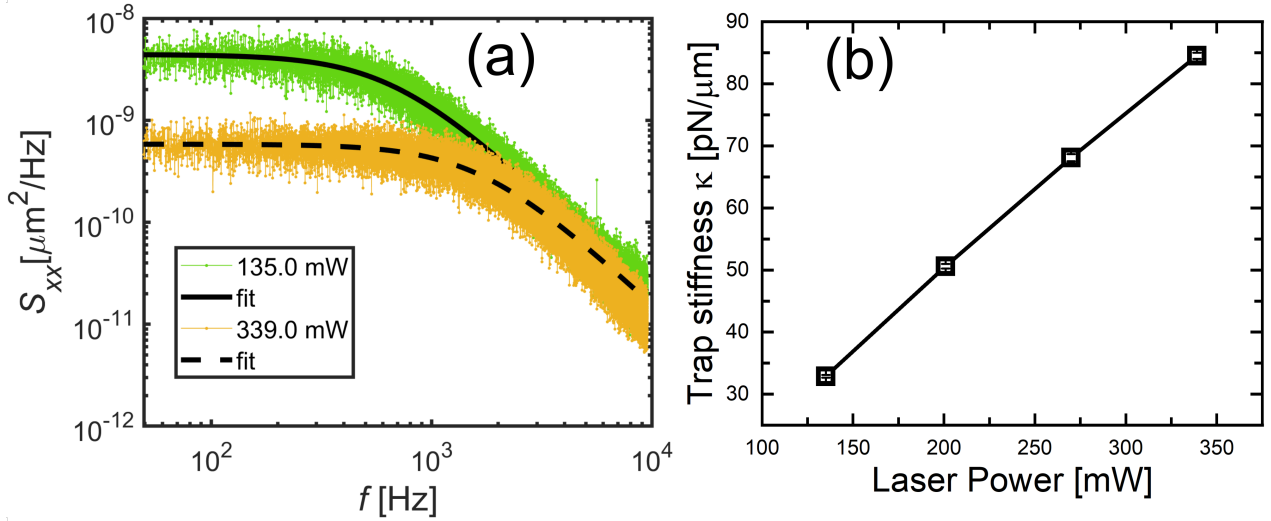


Fig. S5: (a) PSDs for a trapped microsphere in water at two different laser powers and the Lorentzian fits to the data (black lines). (b) Changes in trap stiffness with laser power.

### ST2.3 Calibration of trap stiffness

The stiffness of the optical trap was calculated using the power spectral density method. A Latex microsphere of size  $1\mu\text{m}$  was trapped in water using an optical tweezer at a desired laser power. The microsphere was trapped at approximately  $7\mu\text{m}$  above the bottom surface to eliminate wall effects. The calculated power spectral density,  $S_{xx}(f)$ , of the centre of mass fluctuations of the trapped particle was fitted to a Lorentzian function:

$$S_{xx} = \frac{k_B T}{\pi^2 \gamma (f_c^2 + f^2)}$$

Data and fits for two different laser powers are shown in Fig. S5(a). The corner frequencies  $f_c = k/2\pi\gamma$  were extracted from the fits. Using the fitted value of  $f_c$  and the estimated value of the Stokes drag coefficient,  $\gamma = 6\pi\eta a$ , the trap stiffness  $\kappa$  was determined for four different laser powers. The trap stiffness shows a linear increase with laser power, as shown in Fig. S5(b).